Proton Transfer in the Mechanism of Triosephosphate Isomerase†

Thomas K. Harris, Robert N. Cole, Frank I. Comer, and Albert S. Mildvan*

Department of Biological Chemistry, The Johns Hopkins University School of Medicine, Baltimore, Maryland 21205

Received August 27, 1998

ABSTRACT: Triosephosphate isomerase (TIM) catalyzes the reversible interconversion of dihydroxyacetone phosphate (DHAP) and glyceraldehyde 3-phosphate (GAP), with Glu-165 removing the *pro-R* proton from C1 of DHAP and neutral His-95 polarizing the carbonyl group of the substrate. During the TIM reaction, ∼2% of the *pro-R* tritium from C1 of DHAP is conserved and appears at C2 of GAP [Nickbarg, E. B., and Knowles, J. R. (1988) *Biochemistry 27*, 5939]. In the "classical" mechanism, 98% of the *pro-R* tritium exchanges with solvent from Glu-165 at the intermediate state and the remaining 2% is transferred by Glu-165 to C2 of the same substrate molecule. This intramolecular transfer of tritium is therefore predicted to be independent of DHAP concentration. On the basis of NMR detection of a strong hydrogen bond between Glu-165 and the 1-OH of an analogue of the enediol intermediate [Harris, T. K., Abeygunawardana, C., and Mildvan, A. S. (1997) *Biochemistry 36*, 14661], we have suggested a "criss-cross" mechanism for TIM in which Glu-165 transfers a proton from C1 of DHAP to O2 of the enediol, and subsequently from O1 of the enediol to C2 of the product GAP. Since the *pro-R* proton is transferred to O2 instead of C2 in the criss-cross mechanism, no intramolecular transfer of label from substrate to product would be expected to occur. However, intermolecular transfer of label could occur if the label exchanges from O2 into a group on the protein and is transferred to GAP in subsequent turnovers. The extent of intermolecular tritium transfer in the criss-cross mechanism would be predicted to be dependent on DHAP concentration. The extent of tritium transfer was studied as a function of initial DHAP concentration using DHAP highly tritiated at the *pro-R* position. At 50% conversion to GAP, triphasic tritium transfer behavior was found. For phase 1, between 0.03 and 0.3 mM DHAP, a constant extent of tritium transfer of 1.19 ± 0.03% occurred. For phase 2, between 0.3 and 1.0 mM DHAP, the extent of transfer progressively increased as a function of DHAP concentration to 2.17 ± 0.15%. For phase 3, between 1.0 and 7.0 mM DHAP, the extent of transfer slightly decreased to 1.68 ± 0.17%. In a direct test for intermolecular isotope transfer, doubly labeled [1(*R*)-D,$^{13}C_3$]DHAP and ^{13}C-depleted [1(*R*)-H,$^{12}C_3$]-DHAP were synthesized, mixed in equal amounts, and incubated at 1 mM total DHAP with TIM, GAP dehydrogenase, NAD^+, and arsenate until 50% conversion to 3-phosphoglycerate occurred. Electrospray ionization mass spectral analysis of the stable 3-phosphoglycerate product detected an extent of 1.4 ± 0.4% of intramolecular D transfer from [$^{13}C_3$]DHAP to the $^{13}C_3$ product, but no intermolecular transfer (≤0.02%) of D from [$^{13}C_3$]DHAP to the $^{12}C_3$ product. Hence, the entire transfer of hydrogen from substrate to product is intramolecular, providing no direct support for the criss-cross mechanism in wild-type TIM. The increase in the extent of intramolecular isotopic transfer with increasing initial DHAP concentration indicates site−site interaction in this dimeric enzyme which either (i) slows proton exchange with solvent from Glu-165 at the intermediate state in the classical mechanism or (ii) alters the partitioning of the abstracted proton between transfer to C2 by the classical mechanism or to O2 by the criss-cross mechanism in which no intermolecular transfer of label occurs.

Triosephosphate isomerase (TIM)[1] catalyzes the reversible tautomerization of dihydroxyacetone phosphate (DHAP, **1**) to glyceraldehyde 3-phosphate (GAP, **3**) with Glu-165 removing the *pro-R* proton from C1 of DHAP and neutral His-95 polarizing the carbonyl group of the substrate (*1*−*3*) (Scheme 1). Previous studies have shown that the wild type (*1*, *4*) and the E165D mutant of TIM (*5*) catalyzed the transfer of ∼2% of the tritium label at C1 of DHAP to C2 of the product, GAP, while the H95Q mutant showed no detectable transfer (*2*). These observations were explained by the "classical" mechanism for the wild-type and E165D enzymes in which Glu-165 (or Asp-165) catalyzes intramolecular proton transfer between C1 and C2 and His-95 catalyzes proton transfer between O1 and O2 (Scheme 1). Exchange with solvent is presumed to occur by reversible proton dissociation from Glu-165 at the intermediate state prior to proton transfer to form product. To explain the failure of

† This research was supported by a grant from the National Institutes of Health (DK 28616) to A.S.M. R.N.C. is supported by a grant from the American Health Assistance Foundation to Dr. Gerald Hart. F.I.C. is supported by NIH Grant 2R37-HD13563 to Dr. Gerald Hart.

* To whom correspondence should be addressed.

[1] Abbreviations: TIM, triosephosphate isomerase; DHAP, dihydroxyacetone phosphate; GAP, glyceraldehyde 3-phosphate; PGH, phosphoglycolohydroxamic acid; LBHB, low-barrier hydrogen bond; ϕ, fractionation factor; δ, chemical shift; amu, atomic mass unit; SIM, selected ion monitoring; pH*, pH measured in D_2O; *p*/*s*, extent of tritium transfer; **p**/**s**, extent of deuterium transfer.

10.1021/bi982089f CCC: $15.00
Published on Web 11/05/1998

Scheme 1

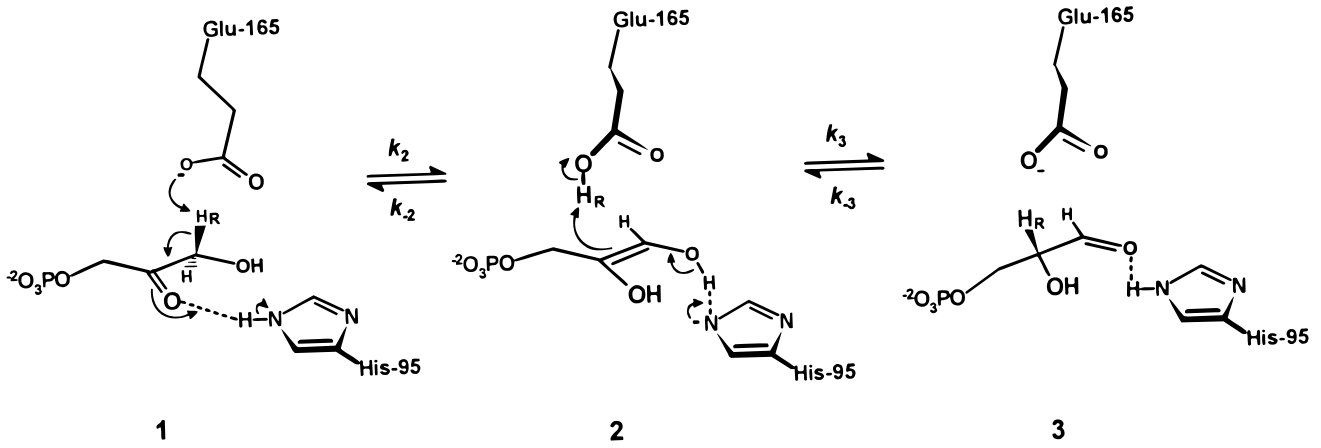

Scheme 2

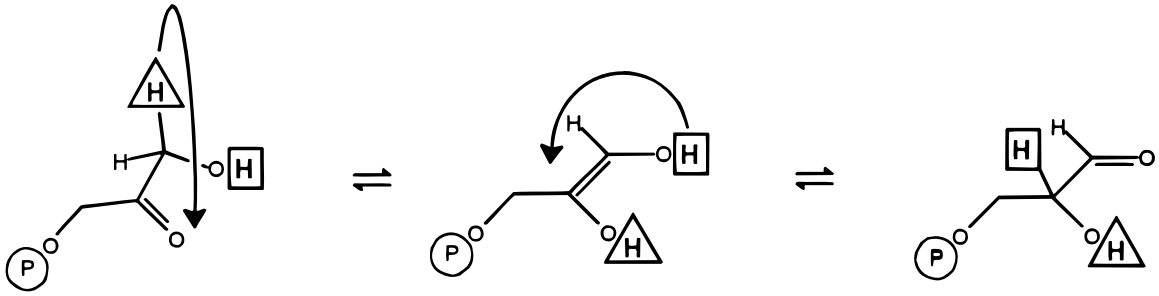

the H95Q mutant to transfer tritium from C1 of DHAP to C2 of GAP, an alternative "criss-cross" mechanism was proposed for the H95Q mutant in which Glu-165 carries out all proton transfer steps as depicted in Scheme 2 (*2*).

In this mechanism, Glu-165 transfers the *pro-R* proton from the C1 position of DHAP to the O2 enediolate oxygen, a solvent exchangeable position, and then from O1, which is also solvent exchangeable, to C2 so that no transfer of tritium from labeled substrate to product is detectable in the H95Q mutant.

Recent one-dimensional and two-dimensional NMR studies of wild-type TIM complexed with phosphoglycolohydroxamic acid (PGH), an analogue of the enediolic intermediate, revealed a low-barrier hydrogen bond (LBHB) between Glu-165 and the 1-NOH proton of PGH ($\delta = 14.9$ ppm, $\phi = 0.38$) and a normal hydrogen bond between His-95 and the 2-carbonyl oxygen of PGH ($\delta = 13.5$ ppm, $\phi = 0.71$) (Figure 1) (*6*). On the basis of the detection of the strong interaction between Glu-165 and the 1-OH of an analogue of the intermediate, we suggested a criss-cross mechanism for wild-type TIM (Scheme 3) which has been modified from the one proposed for the H95Q mutant (Scheme 2) by the addition of a LBHB between Glu-165 and O1 of the intermediate.

The sole operation of the criss-cross mechanism of Schemes 2 and 3 in the wild-type enzyme would require the small amount of tritium transfer from DHAP to GAP to occur in an intermolecular process since all of the label is initially transferred to O2 of the enediolate. In wild-type TIM, a fraction of the *pro-R* tritium label could exchange into the neutral His-95 Nϵ position from O2 in the LBHB-stabilized intermediate at a rate (80 s^{-1})[2] which is 10% of k_{cat} for the conversion of DHAP to GAP (*1*). Hence, ~90% of the

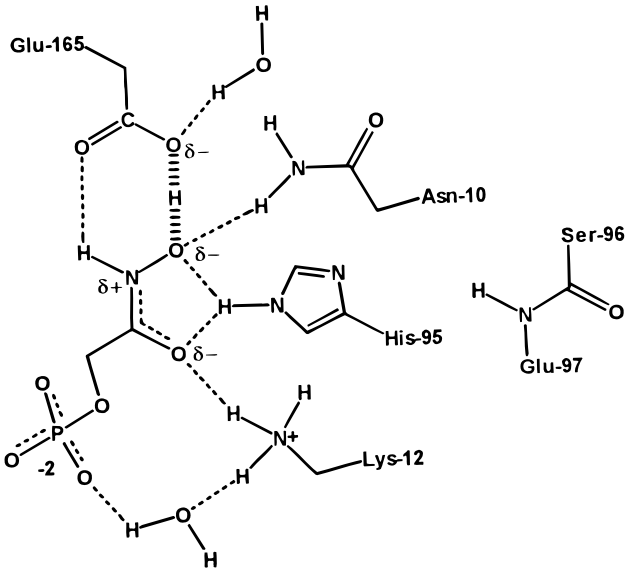

FIGURE 1: NMR-modified X-ray structure of the active site of the TIM−PGH complex showing a strong hydrogen bond between Glu-165 and the 1-NOH of PGH (*3*, *6*, *7*).

tritium would be lost to solvent in the first turnover. In the second turnover, tritium proceeds from His-95 to O1 of the enediol, and then to C2 of the product, again with a 90% loss to solvent resulting in ~1% intermolecular transfer of tritium from DHAP to GAP.

In principle, intermolecular transfer of tritium from substrate to product can be distinguished from intramolecular

[2] The measured rate of exchange of His-95 NϵH with solvent in the TIM−PGH complex (80 s^{-1} at 30 °C) was determined from Arrhenius analysis of the temperature dependence of its line width in ^{1}H NMR spectra (*6*).

Scheme 3

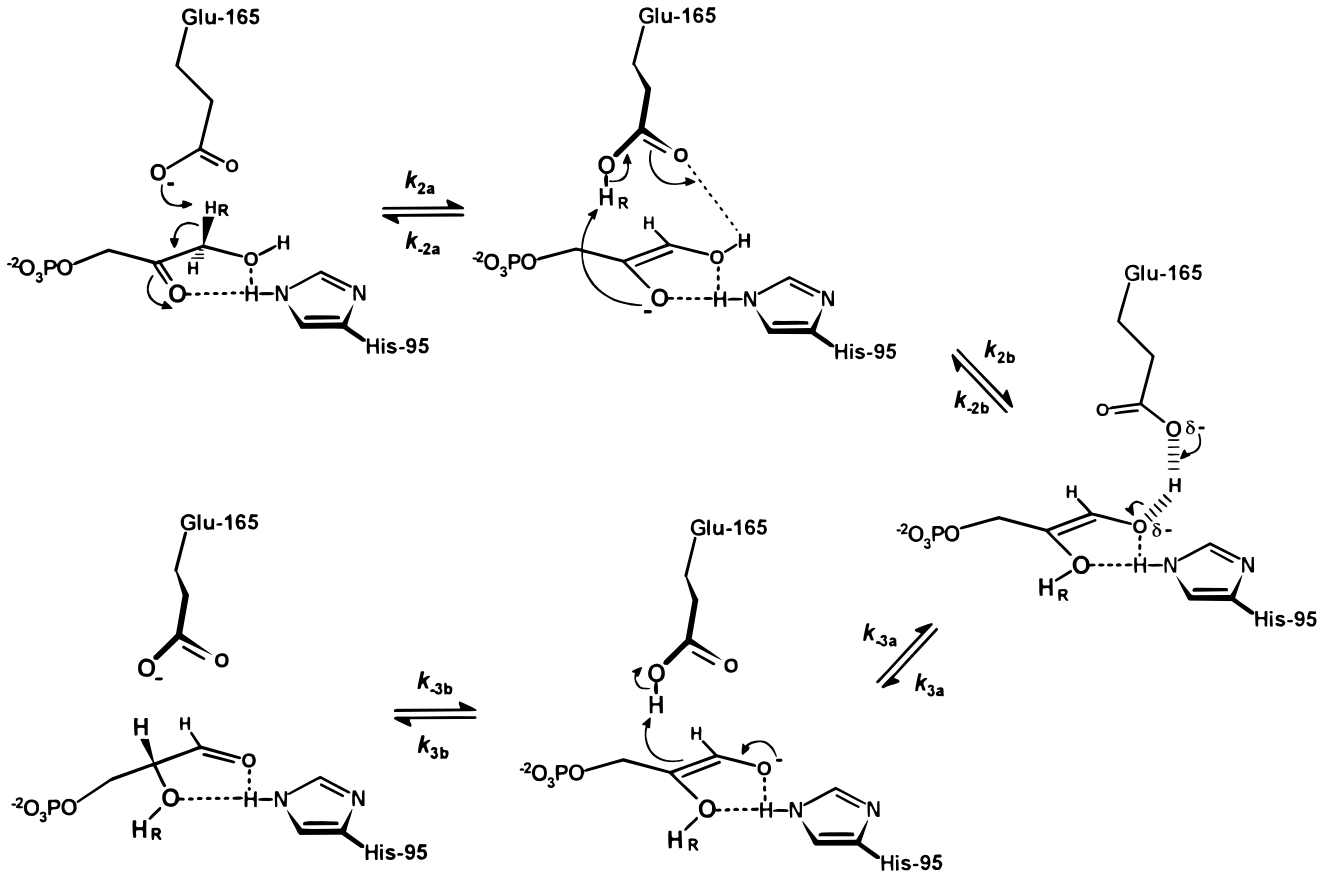

transfer because the extent of intermolecular transfer should be dependent on the initial substrate concentration while that of intramolecular transfer should not be. In this paper, we show that while the extent of transfer of *pro-R* tritium from C1 of DHAP to C2 of GAP is indeed dependent on the initial concentration of DHAP, the entire transfer of label from substrate to product is intramolecular, providing no direct support for the criss-cross mechanism. Hence, the DHAP concentration-dependent intramolecular isotopic transfer indicates site−site interaction in this dimeric enzyme which either (i) slows proton exchange with solvent from Glu-165 at the intermediate state in the classical mechanism or (ii) alters the partitioning of the abstracted proton between transfer to C2 by the classical mechanism or to O2 by the criss-cross mechanism in which no intermolecular transfer of label occurs.

EXPERIMENTAL PROCEDURES

Materials. Aldolase (rabbit muscle), glyceraldehyde-3-phosphate dehydrogenase (rabbit muscle), α-glycerophosphate dehydrogenase (rabbit muscle), hexokinase (yeast), L-lactate dehydrogenase (rabbit muscle), fructose-6-phosphate kinase (*Bacillus stearothermophilus*), phosphoglucose isomerase (yeast), 3-phosphoglycerate kinase (rabbit muscle), and pyruvate kinase (rabbit muscle) were obtained as lyophilized powders, and triosephosphate isomerase (TIM) (yeast) was obtained as a crystalline suspension in ammonium sulfate from Sigma Chemical Co. (St. Louis, MO). Residual TIM contamination was removed from 2 mL preparations of 250 μM sites of aldolase, glyceraldehyde-3-phosphate dehydrogenase, and α-glycerophosphate dehydrogenase by incubation with 10 μM chloroacetol phosphate for 10 min and subsequent purification using a Sephadex G-25 desalting column (17 cm × 1.5 cm) equilibrated in 100 mM triethanolamine-HCl buffer (pH 7.6) and 5 mM EDTA. Yeast TIM was found to be ≥95% pure as determined by 15% SDS−PAGE (*8*) with Coomassie Blue staining and densitometric analysis as well as by its maximum specific activity of 3490 units/mg with DHAP as the substrate, using the assay described below.

Adenosine 5′-triphosphate (ATP, disodium salt), dihydroxyacetone phosphate (DHAP, lithium salt), glyceraldehyde 3-phosphate (GAP, free acid), oxidized nicotinamide adenine dinucleotide (NAD^+), phosphoenolpyruvate (trisodium salt hydrate), 3-phosphoglycerate (disodium salt), reduced nicotinamide adenine dinucleotide (NADH, disodium salt), sodium arsenate, triethanolamine-HCl, triethylammonium bicarbonate buffer, Dowex 1 (Cl^- form, 200−400 mesh, 8% cross-linked), Dowex 50W (H^+ form, 100−200 mesh, 4% cross-linked), and Sephadex G-25 (20−80 μm bead size) were from Sigma Chemical Co. DEAE-cellulose (DE-52) was from Whatman Inc. (Fairfield, NJ). Methanol (GC/GC−MS grade) was from Burdick & Jackson, Inc. (Muskegon, MI). Chloroacetol phosphate diethyl ketal biscyclohexylammonium salt was a gift from F. Hartman. Chloroacetol phosphate, the active form of the inhibitor, was prepared by acid hydrolysis of 5 mL of 50 mM diethyl ketal by the addition of 0.6 g of Dowex 50W-H^+ cation exchange resin and incubating at 40 °C for 48 h, filtering, and neutralizing to pH 4.5 with solid $NaHCO_3$. Acetic acid (double-distilled PPB, Teflon grade) and deuterium oxide (D_2O, 99.96 at. % D) were from Aldrich (Milwaukee, WI).

Scheme 4

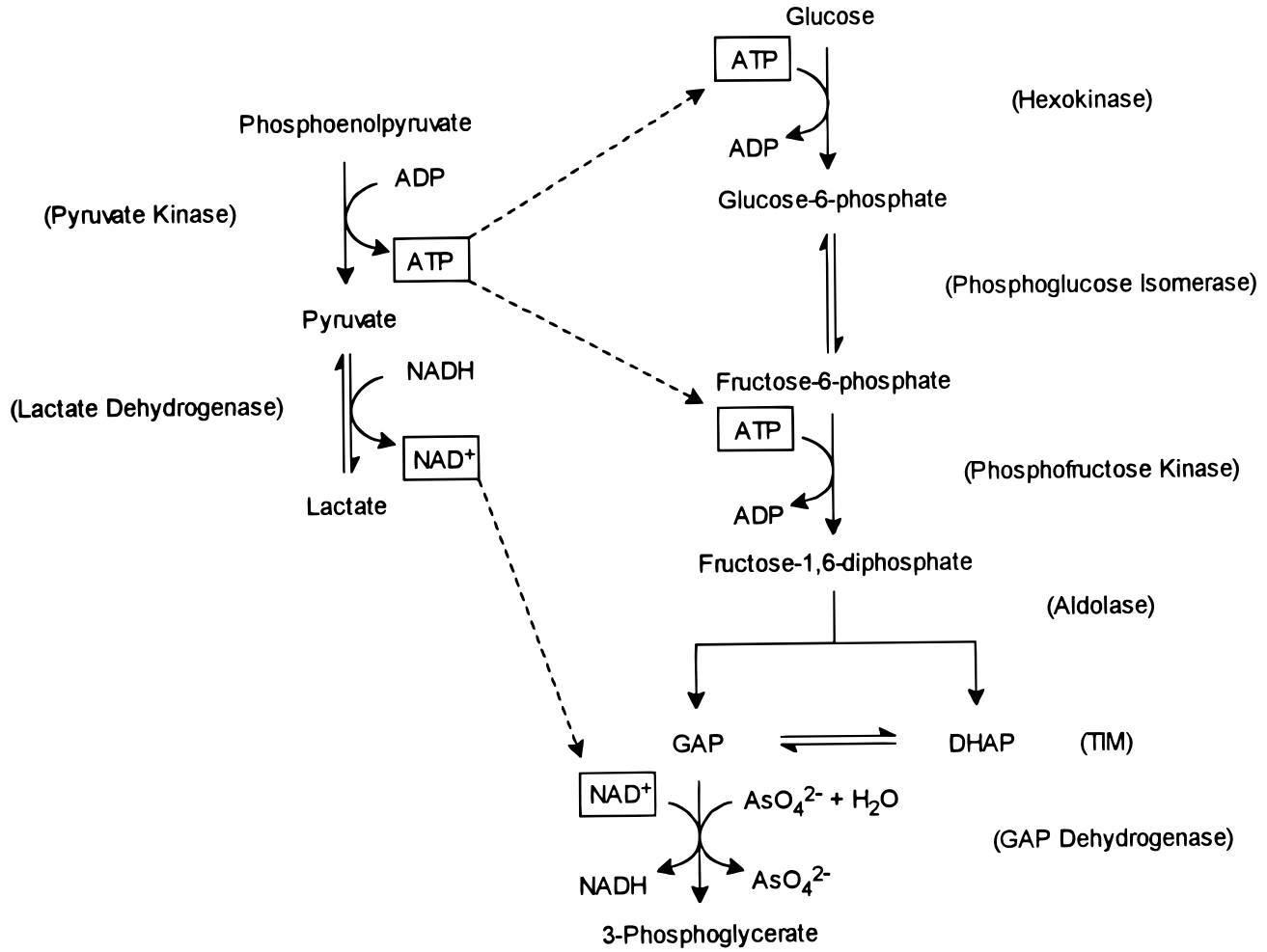

D-[$^{13}C_6$]Glucose (99%) was from Cambridge Isotope (Andover, MA). ^{13}C-depleted D-[$^{12}C_6$]glucose (99.9%) was from Isotec, Inc. (Miamisburg, OH). D-[5-^{3}H]Glucose (17 400 Ci/mol) was from Amersham (Arlington Heights, IL). [^{3}H]-Water (TOH, 5 Ci/mL) was from American Radiolabeled Chemicals, Inc. (St. Louis, MO). [1(*R*)-^{3}H]DHAP (15.3 Ci/mol) was prepared according to Herlihy et al. (*4*) except that the enzymatic labeling reaction mixture was 1 mL of 150 mM triethanolamine-HCl buffer (pH 7.4) containing 100 mM DHAP and 0.5 mg/mL TIM in [^{3}H]H_2O (18.2 Ci/mol). Budget-Solve scintillation cocktail was from Research Products International (Mount Prospect, IL). All solvents and reagents were of analytical or reagent grade and were used without further purification unless otherwise indicated.

General Methods. Protein was analyzed with bicinchoninic acid (*9*) with a bovine serum albumin standard. The solution pH was measured with a Beckman Φ10 pH meter and an Aldrich combination electrode, calibrated with Fisher standard buffer solutions. Samples (500 or 600 μL) for radiochemical analysis were dissolved in scintillation cocktail (7 mL) and counted in a Beckman LS 6000SE automatic liquid scintillation counter. Ultraviolet−visible spectroscopy was performed on a Perkin-Elmer Lambda 9 UV/VIS/NIR spectrophotometer. An extinction coefficient at pH 7.6 for NADH of 6220 M^{-1} cm^{-1} at 340 nm was used.

DHAP and 3-Phosphoglycerate Assays. DHAP was assayed by reduction to glycerol phosphate with α-glycerophosphate dehydrogenase (*10*). The solution contained 200 mM triethanolamine-HCl buffer (pH 7.6), 0.2 mM NADH, and a sample containing 10−150 nmol of DHAP, in a final volume of 1 mL. The reaction was initiated by the addition of 2 units of the dehydrogenase, and the extent of the decrease in absorbance at 340 nm was monitored. 3-Phosphoglycerate was assayed by phosphorylation by phosphoglycerate kinase to 1,3-diphosphoglycerate followed by reductive dephosphorylation with GAP dehydrogenase to GAP (*10*). The solution contained 200 mM triethanolamine-HCl buffer (pH 7.6), 5 mM EDTA, 10 mM $MgCl_2$, 1.6 mM hydrazine-HCl, 6 mM ATP, 0.2 mM NADH, 16 units of GAP dehydrogenase, and a sample containing 10−150 nmol of 3-phosphoglycerate in a final volume of 1 mL. The reaction was initiated by the addition of 2 units of 3-phosphoglycerate kinase, and the extent of the decrease in absorbance at 340 nm was monitored.

Synthesis of [$^{13}C_3$]DHAP and ^{13}C-Depleted [$^{12}C_3$]DHAP. [$^{13}C_3$]DHAP was synthesized from D-[$^{13}C_6$]glucose, and [$^{12}C_3$]-DHAP was synthesized from ^{13}C-depleted D-[$^{12}C_6$]glucose by the following procedure. First, D-[$^{13}C_6$]glucose and ^{13}C-depleted D-[$^{12}C_6$]glucose were converted to [$^{13}C_3$]-3-phosphoglycerate and ^{13}C-depleted [$^{12}C_3$]-3-phosphoglycerate, respectively, making use of the first six steps of glycolysis with irreversible arsenolysis in the final step (Scheme 4).

The overnight conversion occurred at room temperature in a 10 mL reaction mixture containing 100 mM triethanol-

Scheme 5

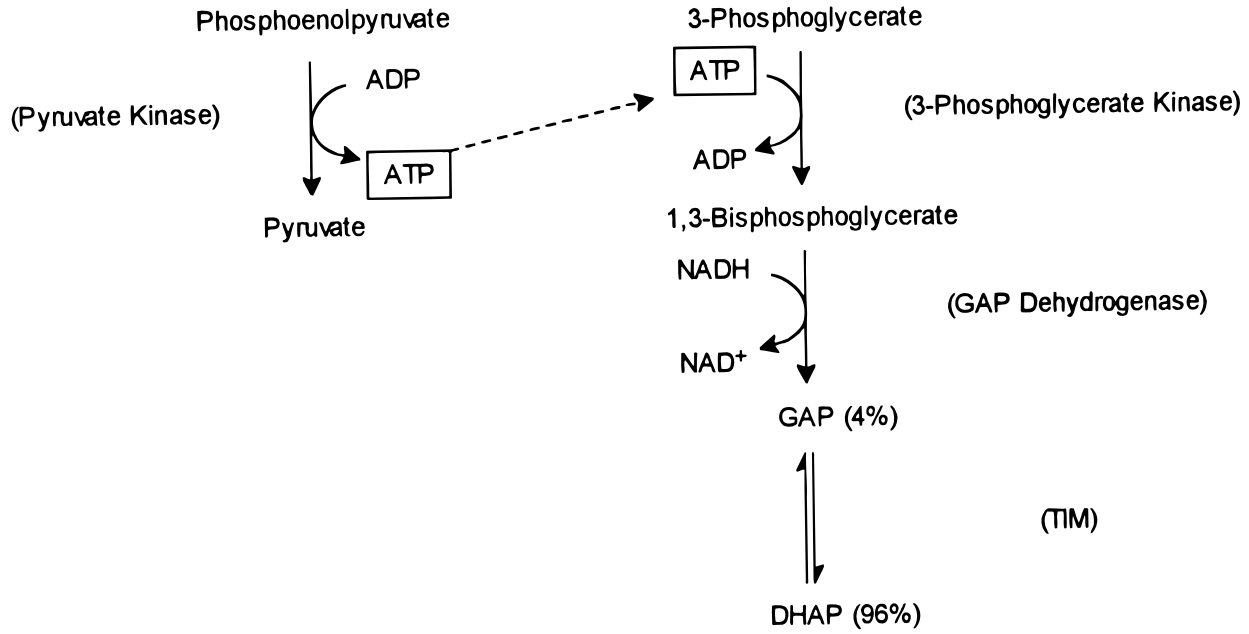

amine-HCl buffer (pH 7.1), 5 mM EDTA, 20 mM $MgCl_2$, 50 mM KCl, 5 mM sodium arsenate, 2 mM NAD^+, 2 mM ATP, 100 mM phosphoenolpyruvate, 50 mM D-[$^{13}C_6$]glucose or ^{13}C-depleted D-[$^{12}C_6$]glucose, 125 units of hexokinase, 100 units of phosphoglucose isomerase, 125 units of phosphofructose kinase, 100 units of aldolase, 250 units of TIM, 250 units of GAP dehydrogenase, 250 units of pyruvate kinase, and 250 units of lactate dehydrogenase. Phosphoenolpyruvate and pyruvate kinase were used to regenerate ATP, and subsequent reduction of pyruvate to lactate by lactate dehydrogenase was used to regenerate NAD^+. The reaction progress was monitored by removing small aliquots of the reaction mixture and assaying for 3-phosphoglycerate as described above. After the reaction mixture reached equilibrium, the enzymes were removed by ultrafiltration through Amicon Centricon-10 concentrators at 5000*g*, and the filtrate was diluted to 800 mL with 5 mM triethanolamine-HCl buffer (pH 7.1), applied to a DEAE-cellulose column (17 cm × 1.5 cm) equilibrated at 4 °C with 5 mM triethanolamine-HCl buffer (pH 7.1), and washed with 200 mL of this buffer (*4*). A linear gradient (80 + 80 mL) of triethanolamine-HCl (5 to 300 mM) was applied to the column, and 2 mL fractions were collected. Since 1 mol of labeled glucose produces 2 mol of labeled 3-phosphoglycerate, the overall yield of ≥400 μmol of 3-phosphoglycerate from 500 μmol of glucose is ≥40%.

Next, fractions containing labeled 3-phosphoglycerate in ∼200 mM triethanolamine-HCl buffer (pH 7.1) were combined (40 mL), and [$^{13}C_3$]-3-phosphoglycerate and ^{13}C-depleted [$^{12}C_3$]-3-phosphoglycerate were converted to [$^{13}C_3$]-DHAP and ^{13}C-depleted [$^{12}C_3$]DHAP, respectively, in a 100 mL overnight room-temperature incubation mixture containing 80 mM triethanolamine-HCl buffer (pH 7.1), 20 mM $MgCl_2$, 50 mM KCl, 10 mM NADH, 0.2 mM ATP, 10 mM phosphoenolpyruvate, 4 mM [$^{13}C_3$]-3-phosphoglycerate or ^{13}C-depleted [$^{12}C_3$]-3-phosphoglycerate, 600 units of 3-phosphoglycerate kinase, 1600 units of GAP dehydrogenase, 1600 units of TIM, and 1600 units of pyruvate kinase (Scheme 5).

The reaction progress was monitored by removing small aliquots of the reaction mixture and assaying for DHAP as described above. After the reaction mixture reached equilibrium, the reaction was quenched by lowering the pH to 3.8 and the mixture was stored as 4−25 mL aliquots at −80 °C until further purification by chromatography. Each 25 mL aliquot was diluted to 250 mL with 0.16 mM HCl (pH 3.8), and the solutions were applied to a Dowex 1-Cl^- column (35 cm × 2.5 cm) equilibrated at 4 °C with 0.16 mM HCl (pH 3.8) and washed with 200 mL of this solution. A nonlinear pH gradient (400 + 400 mL) of HCl (0.16−100 mM) was applied to the column, and 5 mL fractions were collected. Fractions containing [$^{13}C_3$]DHAP or ^{13}C-depleted [$^{12}C_3$]DHAP were pooled, lyophilized, resuspended in a volume of 0.16 mM HCl (pH 3.8) to a final concentration of 40 mM, and stored at −80 °C. A yield of ≥300 μmol of DHAP from 400 μmol of 3-phosphoglycerate was obtained.

Synthesis of [1(R)-D,$^{13}C_3$]DHAP. Since the TIM equilibrium favors DHAP by 24:1 (*4*), [$^{13}C_3$]DHAP was enzymatically labeled with deuterium at the *pro-R* position by incubating a 7 mL reaction mixture containing 100 μmol of [$^{13}C_3$]DHAP with 5000 units of TIM in 100 mM triethanolamine-DCl buffer in D_2O (pH* 7) at room temperature for 2 h. The reaction was quenched by lowering the pH to 3.8 with DCl, and isomerase was removed by ultrafiltration. The filtrate was diluted to 500 mL with 0.16 mM HCl (pH 3.8), and [1(*R*)-D,$^{13}C_3$]DHAP was purified on a Dowex 1-Cl^- column (34 cm × 2.3 cm) as described above. There was no detecable GAP in the purified DHAP, and the extent of deuterium incorporation into DHAP was shown to be ≥80% by electrospray ionization mass spectrometry.

Synthesis of [5-^{3}H]Fructose 1,6-Diphosphate (FDP). D-[5-^{3}H]Glucose (17 400 Ci/mol) and D-glucose were enzymatically converted to [5-^{3}H]FDP (17.4 Ci/mol) using the first three steps of glycolysis (Scheme 4). A 2.5 mL reaction solution contained 100 mM triethanolamine-HCl buffer (pH 7.1), 5 mM EDTA, 20 mM $MgCl_2$, 20 mM ATP, 5 μM D-[5-^{3}H]glucose (17 400 Ci/mol), 5 mM D-glucose, 25 units of hexokinase, 25 units of phosphoglucose isomerase, and 25

units of phosphofructose kinase. The reaction progress was monitored by removing small aliquots of the reaction mixture containing 10−150 nmol of FDP and assaying for FDP by cleavage to GAP and DHAP with aldolase, isomerization of GAP to DHAP with TIM, and reduction to glycerol phosphate with α-glycerophosphate dehydrogenase. The reaction of a 1 mL assay solution containing 100 mM triethanolamine-HCl buffer (pH 7.1), 0.2 mM NADH, 12 units of TIM, and 12 units of glycerophosphate dehydrogenase was initiated by the addition of 2 units of aldolase, and the extent of the decrease in absorbance at 340 nm was monitored. After 1.5 h, 85% of the glucose had been converted to FDP, and the reaction was stopped by removing the enzymes by ultrafiltration through an Amicon Centricon-10 concentrator at 5000*g*. The filtrate was diluted to 100 mL with water, and the pH was lowered to 3.8 with 1 M HCl. This solution was applied to a Dowex 1-Cl^- column (20 cm × 1.5 cm) equilibrated at 4 °C with 0.16 mM HCl (pH 3.8) and washed with 100 mL of this solution. A nonlinear pH gradient (80 + 80 mL) of HCl (0.16 to 150 mM) was applied to the column, and 2 mL fractions were collected. Fractions containing [^{3}H]FDP (17.4 Ci/mol) were pooled, lyophilized, resuspended in a volume of water to a final concentration of 10 mM, and stored at −80 °C.

GAP Dehydrogenase Trapping Efficiency. The efficiency by which GAP dehydrogenase converts [2-^{3}H]GAP to [2-^{3}H]-phosphoglycerate in the coupled enzyme assay for measuring the extent of tritium transfer from [1(*R*)-^{3}H]DHAP to GAP catalyzed by TIM was established as follows. In addition to the standard components used in the coupled enzyme assay mixture containing 100 mM triethanolamine-HCl (pH 7.6), 5 mM EDTA, 5 mM sodium arsenate, 10 mM NAD^+, 0.1−1.0 mM DHAP, 40 units/mL isomerase-free GAP dehydrogenase, and 0.04 unit of TIM, labeled [2-^{3}H]GAP was introduced to the system by the addition of 50 μM [5-^{3}H]-FDP (17.4 Ci/mol) and 0.01 unit of aldolase. As a negative control, aldolase was omitted. Inefficient conversion of [2-^{3}H]GAP to [2-^{3}H]phosphoglycerate by GAP dehydrogenase would result in the TIM-catalyzed exchange of label from [2-^{3}H]GAP to solvent. The 1 mL reaction solutions were mixed and equilibrated at either 5, 30, or 45 °C, and the reactions were initiated by the addition of a mixture of TIM with aldolase (reaction) or TIM without aldolase (control). The extent of the reactions was monitored by taking dilutions of identical reaction mixtures and measuring the absorbance at 340 nm due to the coupled GAP dehydrogenase-catalyzed reduction of NAD^+. After 50% conversion to product, the reactions were quenched by lowering the pH to 3.8 by the addition of 1 M HCl. The amount of radioactivity that was exchanged into solvent was determined by applying the quenched reaction and control mixtures to individual Dowex 1-Cl^- columns (2.5 cm × 0.7 cm) equilibrated in 0.16 mM HCl (pH 3.8). The columns were washed with this same solution, and 0.5 mL fractions were collected. The amount of total radioactivity for both the control and reaction mixtures (≤2000 dpm) was determined from the sum of the radioactivities in the collected fractions for each experiment. As a positive control, the amount of radioactivity released into the solvent in the absence of the GAP dehydrogenase trap was measured.

Extent of Tritium Transfer from [1(R)-^{3}H]DHAP to GAP. The dependence of the extent of isomerase-catalyzed tritium transfer from [1(*R*)-^{3}H]DHAP to GAP on initial DHAP concentration was determined as described by Herlihy et al. (*4*), who made such measurements at only a single concentration of DHAP, with the following additions or modifications. The final reaction mixtures contained 100 mM triethanolamine-HCl buffer (pH 7.6), 5 mM EDTA, 5 mM sodium arsenate, 10 mM NAD^+, 40 units/mL isomerase-free GAP dehydrogenase, 0.04 unit/mL TIM, and 0.03−7.0 mM [1(*R*)-^{3}H]DHAP. The solutions were mixed and equilibrated at 5, 30, or 45 °C, and the reactions were initiated by the addition of isomerase. The final volume for the reaction mixtures containing 0.03−0.3 mM DHAP was 10 mL; the specific radioactivity of [1(*R*)-^{3}H]DHAP was 15.3 Ci/mol, and the extent of the reactions was monitored directly by measuring the increase in absorbance at 340 nm due to the coupled GAP dehydrogenase-catalyzed reduction of NAD^+ with the arsenate-coupled oxidation of GAP to 3-phosphoglycerate. The final volume for the reaction mixtures containing 0.3−7.0 mM DHAP was 1 mL; the specific radioactivity of [1(*R*)-^{3}H]DHAP in these mixtures ranged from 2.2 to 15.3 Ci/mol, and the extents of these reactions were monitored by taking dilutions of identical reaction mixtures with unlabeled DHAP and measuring the absorbance at 340 nm. Little or no contamination (≤0.05%) of the [1(*R*)-^{3}H]DHAP substrate by GAP could be detected upon addition of isomerase-free GAP dehydrogenase to the reaction mixture in the absence of isomerase. The reactions were quenched after 50% conversion to product by lowering the pH to 3.8 by the addition of 1 M HCl and freezing in an ethanol/CO_2 bath.

Tritiated water was removed from the quenched reaction mixtures by twice lyophilizing and then dissolving the resulting residues in 0.16 mM HCl (2 mL). Isomerase and GAP dehydrogenase were then removed by ultrafiltration through Amicon Centricon-10 concentrators at 5000*g*, and the filtrates were stored at −80 °C until they were ready for column chromatography. The mixture of radiolabeled GAP and DHAP in each sample was diluted to 100 mL with 5 mM triethanolamine-HCl buffer (pH 7.1), applied to a DEAE-cellulose column (17 cm × 1.5 cm) equilibrated at 4 °C with 5 mM triethanolamine-HCl buffer (pH 7.1), and washed with 100 mL of this buffer (*4*). A linear gradient (80 + 80 mL) of triethanolamine-HCl (pH 7.1) (5 to 300 mM) was applied to the column; 2 mL fractions were collected, and 4 drops of 1 M HCl was added to each fraction immediately after collection. The yield of DHAP and 3-phosphoglycerate was ≥80%.

The specific radioactivities of DHAP at 0% conversion (s_o) and of both DHAP (s) and 3-phosphoglycerate (p) at 50% conversion were determined by dividing the amount of total radioactivity (after subtraction of background counts) by the amount of DHAP or 3-phosphoglycerate contained in a 600 μL aliquot of fractions containing either DHAP or 3-phosphoglycerate. A 600 μL aliquot typically gave ≤10^6 dpm for fractions containing DHAP, ≤10^4 dpm for fractions containing 3-phosphoglycerate, and ≤10^3 dpm for the background radioactivity which was determined from the average radioactivity in 600 μL aliquots of fractions at the end of the gradient. DHAP and 3-phosphoglycerate were assayed as described above.

Deuterium Transfer from [1(R)-D,$^{13}C_3$]DHAP to GAP. The extent of isomerase-catalyzed deuterium transfer to GAP

from a mixture of doubly labeled [1(*R*)-D,$^{13}C_3$]DHAP and unlabeled ^{13}C-depleted [1(*R*)-H,$^{12}C_3$]DHAP was determined as described above for tritium transfer to GAP with the following additions or modifications. [1(*R*)-D,$^{13}C_3$]DHAP and ^{13}C-depleted [1(*R*)-H,$^{12}C_3$]DHAP were mixed in equal amounts, and the final volume for the reaction mixture containing 1 mM total DHAP was 10 mL. The reaction was quenched after 50% conversion to product by lowering the pH to 3.8 with 1 M HCl. Isomerase and GAP dehydrogenase were removed by ultrafiltration through Amicon Centricon-10 concentrators at 5000*g*, and the sample was stored at −80 °C until it was ready for column chromatography. The quenched reaction mixture was diluted 10-fold with 5 mM triethylammonium bicarbonate (pH 8.5), and the pH was adjusted back to 8.5 with 1 M NaOH. The mixture of 3-phosphoglycerate and DHAP in each sample was applied to a DEAE-cellulose column (17 cm × 1.5 cm) equilibrated with 5 mM triethylammonium bicarbonate (pH 8.5) at 4 °C and washed with 40 mL of 5 mM triethylammonium bicarbonate. A linear gradient (80 + 80 mL) of triethylammonium bicarbonate (5 to 300 mM) was then applied to the column, and 2 mL fractions were collected. The yields of both DHAP and 3-phosphoglycerate were >60%. DHAP and 3-phosphoglycerate were assayed as described above using 200 μL aliquots from the selected fractions. Fractions containing the highest amounts of 3-phosphoglycerate were combined, lyophilized, redissolved in 1 mL of 20% methanol, and assayed as described above. The samples were then prepared for electrospray ionization mass spectrometry by diluting with 20% methanol to obtain 100 μM 3-phosphoglycerate and lowering the pH to 3.8 with double-distilled glacial acetic acid.

Mass Spectrometry. Electrospray ionization mass spectrometry was performed using a Finnigan LCQ atmospheric pressure ionization quadrupole ion trap mass spectrometer equipped with an electrospray ionization probe (ThermoQuest Corp., San Jose, CA). Negative ion mass spectra were obtained using Navigator software version 1.2 (Finnigan MAT, San Jose, CA) on samples injected via a syringe pump at 100 μL/min. Spray conditions consisted of a spray voltage of 3.5 kV, a sheath gas flow rate of 90 (arbitrary) units with no auxiliary gas flow, and a capillary temperature of 219 °C. All other voltages were set by automatic tuning on a 185 atomic mass unit (amu) standard. Data were collected in centroid mode by selected ion monitoring (SIM) of 185, 186, 188, and 189 amu ions (±1 amu) at three microscans during a 500 ms maximum injection time using the automatic gain control for the ion trap and a SIM target number of 2 × 10^7 ions.

RESULTS

Tritium Transfer from [1(R)-^{3}H]DHAP to GAP as a Function of Substrate Concentration and Temperature. The extent of tritium transfer from [1(*R*)-^{3}H]DHAP to GAP after 50% conversion by yeast TIM was studied as a function of initial DHAP concentration (0.03−7.0 mM) and temperature by trapping the [2-^{3}H]GAP product in a coupled reaction with GAP dehydrogenase to form [2-^{3}H]-3-phosphoglycerate. Figure 2 shows the specific radioactivity of the 3-phosphoglycerate product (*p*) (expressed as a percentage of the initial specific radioactivity of DHAP, p/s_o), the specific radioactivity of the remaining DHAP substrate (*s*) (expressed as the fraction of s_o, s/s_o), and the percentage of tritium transfer to GAP (p/s), each plotted against initial DHAP concentration for the reaction of DHAP with yeast TIM at 30 °C. These data can be divided into three distinct phases. The first phase showed a constant amount of tritium transfer to GAP occurring between 0.03 and 0.3 mM DHAP with an average p/s value of 1.19 ± 0.03%. This constant value results from the ratio of values of p/s_o and s/s_o that slightly decreased over this range by similar magnitudes. The second phase showed an increase in tritium transfer between 0.3 and 1.0 mM DHAP with a maximum p/s of 2.17 ± 0.15%. The increase in p/s results from increased values of p/s_o, while s/s_o continued to decrease over this range. The third phase showed a slight decrease in tritium transfer between 1.0 and 7.0 mM DHAP with a p/s value of 1.68 ± 0.17%. This decrease results from s/s_o increasing by a slightly greater magnitude than the increase in p/s_o over this range. At 30 °C and a single DHAP concentration of 2.0 mM, under otherwise identical conditions, Knowles and co-workers obtained p/s values of 1.64 and 2.16% with yeast TIM (*1*) and chicken muscle TIM (*4*), respectively, in agreement with the values in phase 3 of our DHAP titration of yeast TIM.

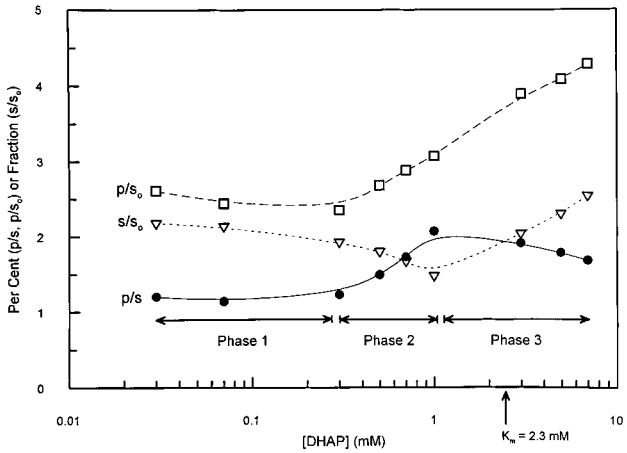

FIGURE 2: Extent of tritium transfer from DHAP to GAP vs initial DHAP concentration. The specific radioactivity of the 3-phosphoglycerate product expressed as a percentage of the initial specific radioactivity of DHAP (□), the specific radioactivity of the remaining DHAP substrate expressed as the fraction of of the initial specific radioactivity of DHAP (▽), and the percentage of tritium transfer to GAP (●), in which the specific radioactivity of the 3-phosphoglycerate product is expressed as a percentage of the specific radioactivity of the remaining DHAP substrate, are plotted vs initial DHAP concentration for the reaction of DHAP with TIM at 30 °C.

To determine whether this variation in the extent of tritium transfer with DHAP concentration might have been an artifact resulting from an increase in the efficiency of trapping of [2-^{3}H]GAP at higher substrate concentrations, a test of the trapping efficiency by GAP dehydrogenase was carried out. Inefficient conversion of [2-^{3}H]GAP to [2-^{3}H]-3-phosphoglycerate by GAP dehydrogenase would result in TIM-catalyzed exchange of the label from [2-^{3}H]GAP to solvent. Although the validity of using GAP dehydrogenase in the coupled enzyme assay for DHAP has previously been established by showing that the observed rate of reduction of NAD^+ truly represents the rate of the TIM-catalyzed isomerization of DHAP to GAP (*11*), we further tested the GAP dehydrogenase trapping efficiency by a more sensitive method. In addition to the standard components used in the

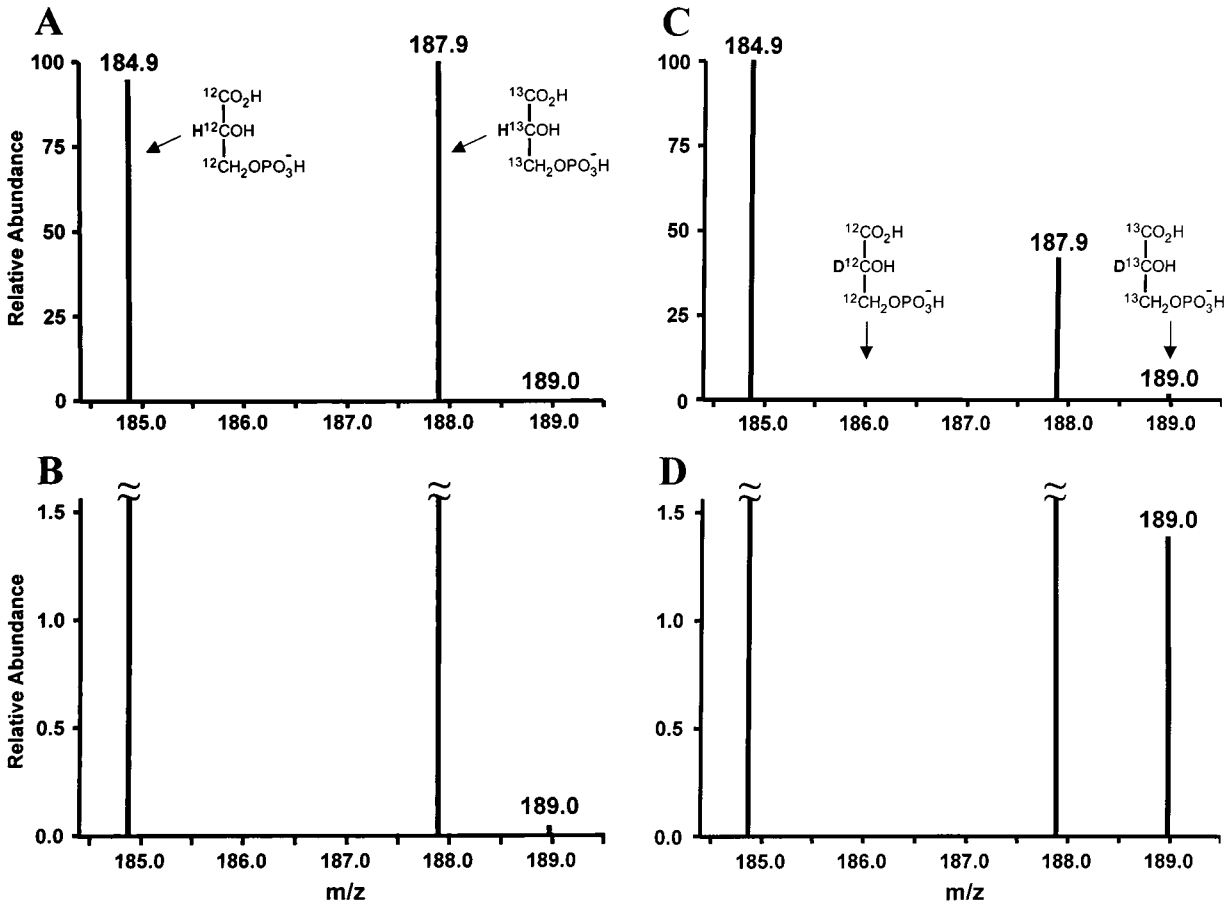

FIGURE 3: Test for intermolecular deuterium transfer from [^{13}C]DHAP to [^{12}C]GAP catalyzed by TIM. (A) Mass spectrum of the 3-phosphoglycerate isotopic products for the control reaction. The peaks at *m*/*z* 184.9 and 187.9 correspond to [2-H,$^{12}C_3$]-3-phosphoglycerate and [2-H,$^{13}C_3$]-3-phosphoglycerate, respectively. (B) Enlarged scale of the mass spectrum of the 3-phosphoglycerate isotopic products for the control reaction. (C) Mass spectrum of the 3-phosphoglycerate isotopic products for the double-label reaction. The peaks at *m*/*z* 184.9 and 187.9 correspond to [2-H,$^{12}C_3$]-3-phosphoglycerate (77.2 ± 6.2%) and [2-H,$^{13}C_3$]-3-phosphoglycerate (21.6 ± 6.5%), respectively, and the small peak at *m*/*z* 189.0 corresponds to [2-D,$^{13}C_3$]-3-phosphoglycerate (1.1 ± 0.3%). (D) Enlarged scale of the mass spectrum of the 3-phosphoglycerate isotopic products for the double-label reaction.

coupled enzyme assay for measuring the extent of tritium transfer from [1(*R*)-^{3}H]DHAP to GAP catalyzed by TIM (see Experimental Procedures), labeled [2-^{3}H]GAP was introduced into the system by the addition of 10^6 dpm of [5-^{3}H]-FDP and aldolase. A control for each reaction condition contained the standard components used in the coupled enzyme assay with 10^6 dpm of [5-^{3}H]FDP but no aldolase. After 50% conversion of DHAP to 3-phosphoglycerate, few or no disintegrations per minute (<0.002%) were found in the solvent compared to that of the control over the range of conditions used in this study. As a positive control, all disintegrations per minute were found in the solvent for the reaction carried out in the absence of GAP dehydrogenase. Hence, GAP dehydrogenase is effectively 100% efficient in trapping [2-^{3}H]GAP as [2-^{3}H]-3-phosphoglycerate under all conditions used in this study and is no cause for variation in the results.

The extent of tritium transfer for the reaction of yeast TIM with 1.0 mM DHAP increased with decreasing temperature, showing values for *p*/*s* of 1.08 ± 0.07% at 45 °C, 2.07 ± 0.23% at 30 °C, and 3.89 ± 0.43% at 5 °C. The increase in *p*/*s* between 45 and 30 °C results from a decreased value of s/s_o (2.90 ± 0.15% at 45 °C and 1.48 ± 0.08% at 30 °C) while p/s_o remained constant (3.11 ± 0.19% at 45 °C and 3.07 ± 0.29% at 30 °C). The further increase in *p*/*s* between 30 and 5 °C results from the increased value of p/s_o at 5 °C of 7.53 ± 0.82% while s/s_o at 5 °C only slightly increased to 1.93 ± 0.06%.

Deuterium Transfer from [1(R)-D,$^{13}C_3$]DHAP to GAP. To determine whether the 1.1−3.9% transfer of tritium from substrate to product (*p*/*s*) under various conditions results from either (i) intramolecular transfer from C1 to C2 of the same substrate molecule or (ii) intermolecular transfer in which a fraction of the *pro-R* tritium label from substrate is exchanged into a group on the protein and is then transferred to a different carbon skeleton of the product in subsequent turnovers, electrospray ionization mass spectrometry (EIMS) was used to follow the extent of transfer of deuterium from DHAP to product. Doubly labeled [1(*R*)-D,$^{13}C_3$]DHAP and ^{13}C-depleted [1(*R*)-H,$^{12}C_3$]DHAP were synthesized, mixed in equal amounts, and incubated at a total DHAP concentration of 1 mM with TIM, GAP dehydrogenase, NAD^+, and arsenate until 50% conversion to 3-phosphoglycerate occurred. A control reaction with 1(*R*)-protonated rather than deuterated [$^{13}C_3$]DHAP was also performed under otherwise identical conditions.

Figure 3A shows a representative mass spectrum of the 3-phosphoglycerate isotopic products for the control reaction which showed intense peaks with a similar magnitude at *m*/*z* 184.9 corresponding to [2-H,$^{12}C_3$]-3-phosphoglycerate and *m*/*z* 187.9 corresponding to [2-H,$^{13}C_3$]-3-phosphoglycerate. An enlarged scale of this spectrum is shown in Figure 3B

which shows background signals that were ≤0.02% of the total signal near *m*/*z* 186 and 189. Figure 3C shows a representative mass spectrum of the 3-phosphoglycerate isotopic products for the double-label reaction which showed intense peaks at *m*/*z* 184.9 corresponding to [2-H,$^{12}C_3$]-3-phosphoglycerate (77.2 ± 6.2%) and *m*/*z* 187.9 corresponding to [2-H,$^{13}C_3$]-3-phosphoglycerate (21.6 ± 6.5%). The increased relative abundance of [2-H,$^{12}C_3$]-3-phosphoglycerate with respect to [2-H,$^{13}C_3$]-3-phosphoglycerate results from a primary deuterium kinetic isotope effect of 4.0 ± 0.3 in which the reaction rate of [1(*R*)-D,$^{13}C_3$]DHAP is decreased relative to that of [1(*R*)-H,$^{12}C_3$]DHAP.[3] Figure 3C, with an enlarged scale in Figure 3D of this mass spectrum, showed an additional peak at *m*/*z* 189.0 with a 1.1 ± 0.3% relative abundance corresponding to [2-D,$^{13}C_3$]-3-phosphoglycerate. No signals above background (≤0.02%) were observed near *m*/*z* 186 which would correspond to [2-D,$^{12}C_3$]-3-phosphoglycerate. Hence, the entire transfer of deuterium (and tritium) from substrate to product is intramolecular.

The extent of deuterium transfer (**p**/**s**) of 1.42 ± 0.40% was calculated by dividing the relative abundance for the *m*/*z* 189.0 peak, which represents the fraction of [2-D,$^{13}C_3$]-3-phosphoglycerate (**p** = 1.1 ± 0.3%), by the fraction of [1(*R*)-D,$^{13}C_3$]DHAP remaining after 50% conversion (**s** = 0.772 ± 0.062). The fraction of [1(*R*)-D,$^{13}C_3$]DHAP remaining after 50% conversion (**s**) was obtained from the relative abundance for the *m*/*z* 185 peak, which represents [2-H,$^{12}C_3$]-3-phosphoglycerate, since the relative abundances of the [2-H,^{13}C]-3-phosphoglycerate and [2-H,^{12}C]-3-phosphoglycerate products are inversely related to the relative abundances of the corresponding [2-D,^{13}C]DHAP and [2-H,^{12}C]DHAP substrates. The extent of deuterium transfer of 1.4 ± 0.4% is comparable to the value of 2.17 ± 0.15% tritium transfer under these conditions.

DISCUSSION

The notion that the small amount of tritium transfer from DHAP to GAP shown in Figure 2 may have occurred in an intermolecular process is clearly ruled out by the results of Figure 3. The observation of 1.4% intramolecular transfer of deuterium and 1.1−3.9% transfer of tritium from substrate to product under various conditions provides direct evidence that the classical mechanism occurs with a frequency of at least 1.1−3.9% with yeast TIM. However, it is not possible to distinguish what mechanistic pathway is followed for the remaining 96.1−98.9% of the reaction in which the *pro-R* label is ultimately transferred to solvent. The following two limiting cases can explain these data. At one extreme, the classical mechanism (Scheme 1) occurs 100% of the time in which Glu-165 transfers the abstracted *pro-R* label from DHAP to GAP with 1.1−3.9% efficiency and exchange of the label to solvent occurs from Glu-165 at the intermediate state. This is the simplest mechanism. To permit this facile exchange with solvent, at least one proton donor and one proton acceptor must be in proximity to Glu-165 in the enzyme−intermediate complex. At the other extreme, the classical mechanism occurs only 1.1−3.9% of the time with 100% efficiency in transfer of the label and a second predominant pathway such as the criss-cross mechanism (Scheme 3) occurs the remainder of the time with 0% efficiency in conserving the isotopic label because the *pro-R* proton is transferred to the enediolate oxygen, a solvent exchangeable position. Although this explanation is more complex, requiring the participation of two pathways, the transfer of label to both product and solvent can be explained by known groups in the active site and by simple pK_a arguments (see below). Intermediate cases in which the classical and criss-cross mechanisms contribute more equally to catalysis may apply. Thus, with chicken muscle TIM, the classical mechanism must contribute at least 12.1% to catalysis as judged by the reported amount of deuterium transfer from substrate to product at 23% reaction (*12*).

To explain the loss of label from Glu-165 to solvent for the case in which the classical mechanism (Scheme 1) operates 100% of the time, solvation requirements for the catalytic groups in the enzyme−intermediate complex must be described. In the simplest case, Glu-165 exchanges its label with one or more water molecules. These water molecules may or may not be readily accessible to bulk solvent. If rapid exchange with bulk solvent occurred, the small percentage of transfer reflects the kinetic partitioning between exchange with solvent and transfer to C2. A difficulty with a mechanism involving direct proton exchange with solvent from Glu-165 has been pointed out by Rose et al. (*13*), who noted that the loss of such a proton to solvent from the intermediate state, in the classical mechanism, imposes limits on the overall catalytic rate depending on the pK_a of the catalytic base and the pH of the medium. Rose et al. proposed an alternative mechanism for TIM in which the enzyme itself, not the medium, provides a pool of protons with which the enzyme−enediolic intermediate can exchange (internal exchange). Exchange of this enzymic pool with the medium (external exchange) was proposed to occur after the substrate or product had dissociated.

If water molecules were trapped in the active site so that they fully equilibrated with the labeled Glu-165, the retention of only 1.1−3.9% of the label in the product would require dilution of the label among 13−45 trapped water molecules, an unrealistically large number. With the chicken muscle enzyme, where 12.1% of the deuterium was retained (*12*), four trapped water molecules would be required if equilibration were complete. The X-ray structure of the TIM−PGH complex reveals only two water molecules bound in the active site (Figure 1) (*7*), although this is clearly a lower limit since solvent exchangeable water molecules would likely be undetected by X-ray crystallography. The presence of nearby solvent molecules, required by the classical mechanism, could also be counterproductive in that desolvation of Glu-165 must occur for the proper approach and alignment of the carboxylate oxygen syn orbital with the *pro-R* proton of enzyme-bound DHAP. Alternatively, Glu-165 could exchange the *pro-R* proton of DHAP with a solvent-exchangeable residue on the protein. However, the X-ray structure of the TIM−PGH complex (Figure 1) (*7*) shows that the only solvent-exchangeable residue within hydrogen bonding distance of Glu-165 is neutral His-95 which has been proposed to relay protons between O1 and O2 (Scheme 1). Exchange would have to occur from Glu-165 to the very unstable imidazolate anion. Since neutral

[3] This value is very similar to the reported deuterium kinetic isotope effect on both k_{cat} and k_{cat}/K_m of the yeast enzyme of 3.4 ± 0.1 (*1*).

His-95 containing the abstracted *pro-R* proton would then not be able to deprotonate O1, Glu-165 could transfer the O1 proton to C2 as in the criss-cross mechanism (Scheme 3).

Exchange of the *pro-R* label of DHAP with solvent can be rationalized for the case in which the criss-cross mechanism (Scheme 3) makes a significant, but not total, contribution to catalysis. The first step in the mechanisms of Schemes 1 and 3 is abstraction of the *pro-R* proton from C1 of DHAP by Glu-165 with neutral His-95 polarizing the substrate carbonyl group. Concertedly or subsequently, the enediolate O2 oxygen ($pK_a \leq 14$) must be protonated. The X-ray structure of the TIM−PGH complex (Figure 1) (*7*) shows that the only potential acid catalysts within hydrogen bonding distance of O2 at the intermediate state are neutral His-95 ($pK_a \leq 14$) and Glu-165 ($pK_a \leq 7$). The much lower pK_a of Glu-165 and its proximity to O2 make it the thermodynamically more favored donor of a proton to O2. While the proximity of His-95 to O2 makes it competitive with Glu-165 as the proton donor, the pK_a of the neutral form of His-95 closely matches that of the enediolate oxygen so that protonation of O2 is isoenergetic and thermodynamically much less favorable for full proton transfer than that by Glu-165. More likely, the similar pK_a's between neutral His-95 and the enediolate oxygen indicate that a strong hydrogen bond could be transiently formed in which the neutral His-95 proton is only partially transferred to O2 in the transition state for abstraction of the *pro-R* proton by Glu-165, and the free energy of formation of this hydrogen bond could help facilitate such catalysis. These simple considerations are consistent with ab initio quantum mechanical calculations which concluded that deprotonation of His-95 is energetically unfavorable and that the energetically most favorable reaction pathway involves transfer of the abstracted *pro-R* proton to the carbonyl oxygen of the substrate, either directly or after it has exchanged with solvent, producing the enediol intermediate (*14*).

If there is partitioning between the classical and criss-cross mechanisms governed by the pK_a difference between Glu-165 and His-95, then one could postulate that if the pK_a of His-95 was decreased relative to the pK_a of Glu-165 at the intermediate state, then His-95 could more readily protonate O2 so that more transfer of the abstracted *pro-R* label from Glu-165 to C2 of the product would occur. Because nitrogen-containing bases such as imidazole have considerable heats of ionization whereas oxygen-containing bases such as carboxylates have very small heats of ionization, increasing the temperature could provide a method for decreasing the pK_a of His-95 relative to that of Glu-165, resulting in an increased extent of tritium transfer to C2. However, the significant decrease in the extent of tritium transfer upon increasing the temperature from 5 to 45 °C seems to be more characteristic of the classical mechanism in which the rate of exchange of the abstracted *pro-R* label from Glu-165 with solvent increases more with increasing temperature relative to the rate of transfer of the label to C2 of the intermediate.

Although the entire transfer of *pro-R* tritium from C1 of DHAP to C2 of GAP is intramolecular, the extent of transfer is dependent on the initial concentration of DHAP, indicating site−site interaction in this dimeric enzyme. Although there is no previous evidence for cooperativity between the two subunits, only the dimer possesses isomerase activity (*15*). The two active centers and the subunit interfaces are in close contact via an interdigitating loop that extends from one subunit to the other near the active site pockets. Other evidence for interactions between the catalytic centers and the subunit contact sites comes from physical studies both in solution (*16*) and in the crystalline state (*17*) which show a substantial conformational change accompanying the binding of substrate. Although the nature of the cross-talk occurring between the two active sites is subtle since the overall isomerase activity does not change, it inherently reflects details of the mechanisms occurring at the intermediate state. The increase in the extent of tritium transfer from substrate to product upon increasing occupancy from a single site to both sites with DHAP results from site−site interaction which either (i) slows proton exchange with solvent from Glu-165 at the intermediate state in the classical mechanism or (ii) alters the partitioning of the abstracted proton between transfer to C2 by the classical mechanism or to O2 by the criss-cross mechanism in which no intermolecular transfer of label occurs. In principle, this phenomenon can be tested further by performing the DHAP concentration-dependent tritium transfer experiments using a heterodimeric TIM in which one of the subunits has been irreversibly inactivated with the affinity label 3-chloroacetol phosphate (*18*).

CONCLUSIONS

The TIM-catalyzed transfer of 1.4 ± 0.4% of the deuterium from DHAP to GAP is here found to be entirely intramolecular. Hence, this transfer cannot be due to the operation of the criss-cross mechanism (Scheme 3). If it is assumed that intramolecular tritium transfer occurs as well, the classical mechanism (Scheme 1), depending on its efficiency in conserving and transferring tritium, contributes at least 3.9% to the reaction catalyzed by yeast TIM and at least 12.1% to the reaction catalyzed by chicken muscle TIM. If it is inefficient in conserving and transferring tritium, the classical mechanism could contribute up to 100% to catalysis. However, from the structure of the active site of TIM based on X-ray (*7*) and NMR studies (*3*, *6*) (Figure 1), it is possible that the TIM reaction partitions down two pathways depending on competition in the protonation of O2 of the enediolate intermediate by either His-95 in the classical mechanism (Scheme 1) or by Glu-165 in the criss-cross mechanism (Scheme 3). The thermodynamically downhill transfer of the abstracted *pro-R* proton from Glu-165 to the enediolate oxygen favors a significant contribution from the criss-cross mechanism which does not transfer label to product. When His-95 is replaced by Gln, the classical mechanism becomes inoperative and the criss-cross mechanism takes over at 0.7% of the wild-type rate (*2*).

The 2-fold dependence of the extent of intramolecular tritium transfer on the concentration of DHAP indicates, for the first time, site−site interaction in this dimeric enzyme which either (i) slows proton exchange with solvent from Glu-165 at the intermediate state via the classical mechanism or (ii) alters the partitioning of the abstracted proton between transfer to C2 via the classical mechanism or to O2 via the criss-cross mechanism.

ACKNOWLEDGMENT

We thank Dr. Irwin A. Rose for suggesting the GAP dehydrogenase trapping efficiency experiment and for valuable discussions and Dr. Gerald Hart for use of the electrospray ionization mass spectrometer.

REFERENCES

1. Nickbarg, E. B., and Knowles, J. R. (1988) *Biochemistry 27*, 5939−5947.
2. Nickbarg, E. B., Davenport, R. C., Petsko, G. A., and Knowles, J. R. (1988) *Biochemistry 27*, 5948−5960.
3. Lodi, P. J., and Knowles, J. R. (1991) *Biochemistry 30*, 6948−6956.
4. Herlihy, J. M., Maister, S. G., Albery, W. J., and Knowles, J. R. (1976) *Biochemistry 15*, 5601−5607.
5. Raines, R. T., Sutton, E. L., Straus, D. R., Gilbert, W., and Knowles, J. R. (1986) *Biochemistry 25*, 7142−7154.
6. Harris, T. K., Abeygunawardana, C., and Mildvan, A. S. (1997) *Biochemistry 36*, 14661−14675.
7. Davenport, R. C., Bash, P. A., Seaton, B. A., Karplus, M., Petsko, G. A., and Ringe, D. (1991) *Biochemistry 30*, 5821−5826.
8. Laemmli, U. K. (1970) *Nature 227*, 680−685.
9. Smith, P. K., Krohn, R. I., Hermanson, G. T., Mallia, A. K., Gartner, F. H., Provenzano, M. D., Fujimoto, E. K., Goek, N. M., Olson, B. J., and Klenk, D. C. (1985) *Anal. Biochem. 150*, 76.
10. Maister, S. G., Pett, C. P., Albery, W. J., and Knowles, J. R. (1976) *Biochemistry 15*, 5607−5612.
11. Plaut, B., and Knowles, J. R. (1972) *Biochem. J. 129*, 311−320.
12. Fisher, L. M., Albery, W. J., and Knowles, J. R. (1976) *Biochemistry 15*, 5621−5626.
13. Rose, I. A., Fung, W.-J., and Warms, J. V. B. (1990) *Biochemistry 29*, 4312−4317.
14. Peräkylä, M., and Pakkanen, T. A. (1996) *Proteins 25*, 225−236.
15. Lolis, E., Alber, T., Davenport, R. C., Rose, D., Hartman, F. C., and Petsko, G. A. (1990) *Biochemistry 29*, 6609−6618.
16. Sampson, N. S., and Knowles, J. R. (1992) *Biochemistry 31*, 8488−8494.
17. Lolis, E., and Petsko, G. A. (1990) *Biochemistry 29*, 6619−6625.
18. Schnackerz, K. D., and Gracy, R. W. (1991) *Eur. J. Biochem. 199*, 231−238.

BI982089F